

Aerodynamic Behavior of a Compound Wing Configuration in Ground Effect

Saeed Jamei^a, Adi Maimun^{a*}, Shuhaimi Mansor^b, Agoes Priyanto^a, Nor Azwadi^c, M. Mobassher Tofa^a

^aDepartment of Marine Technology, Faculty of Mechanical Engineering, Universiti Teknologi Malaysia, 81310 UTM Johor Bahru, Johor, Malaysia

^bDepartment of Eeronautical Engineering, Faculty of Mechanical Engineering, Universiti Teknologi Malaysia, 81310 UTM Johor Bahru, Johor, Malaysia

^cDepartment of Termo. Fluids, Faculty of Mechanical Engineering, Universiti Teknologi Malaysia, 81310 UTM Johor Bahru, Johor, Malaysia

*Corresponding author: adi@fkm.utm.my

Article history

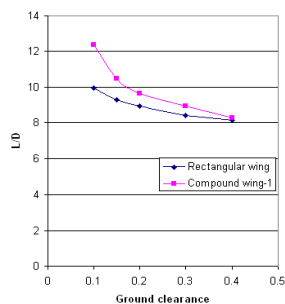
Received :1 August 2013

Received in revised form :

15 November 2013

Accepted :5 December 2013

Graphical abstract



Abstract

The aerodynamic coefficients of wing in ground effect can be affected with its design which can be the main parameter for efficiency of wing-in-ground effect craft. In this study, the aerodynamic coefficients of a compound wing were numerically determined in ground effect. The compound wing was divided into three parts with one rectangular wing in the middle and two reverse taper wings with an anhedral angle at the sides. An NACA6409 airfoil was employed as a section of wings. Three dimensional (3D) computational fluid dynamics (CFD) was applied as a numerical scheme. A realizable $k-\epsilon$ turbulent model was used for simulation the turbulent flow around the wing surfaces. For validation purpose, the numerical results of a compound wing with aspect ratio 1.25, at ground clearance of 0.15 and different angles of attack were compared with the current experimental data. Then, the aerodynamic coefficients of the compound wings were computed at various ground clearances and angle of attack of 4° . According to pressure and velocity distribution of air around wing surfaces, ground clearance had considerable effects on ram effect pressure and tip vortex of the compound wing, and aerodynamic coefficients of the compound wing had some improvements as compared with the rectangular wing.

Keywords: Aerodynamic coefficients; cfd simulation; compound wing; wind tunnel, wing-in-ground effect

© 2014 Penerbit UTM Press. All rights reserved.

1.0 INTRODUCTION

Recently, many countries started to work on WIG crafts and developed because of their advantages such as fuel saving, high speed compared to other water vehicles transport. The study on configuration of WIG crafts experimentally and theoretically is investigated to improve their aerodynamic performance. The principal means to develop lifting force is the ram effect; lift is improved when flow underneath the wing body around stagnation point on the pressure surface (lower surface of body) is trapped. The gathering of high pressure on lower surface and low pressure on upper surface of the body provides a high lifting force which is increased the source of supporting.

Two phenomena influence on aerodynamic characters of wing when a wing approaches to the ground. These are called span dominated and chord dominated ground effect. The main parameter related to span dominated ground effect is h/b (height-to-span ratio) and for chord dominated ground effect is h/c (height-to-chord ratio). The span dominated ground effect causes a reduction in drag force. There are two main source drags for aircraft which are called the viscous drag and induced drag. The viscous drag is created by friction between the air and surface of the aircraft; hence it depends on wetted area. The

induced drag is related to generation of lift. Positive lift is generated when the static pressure on pressure side (lower surface) is greater than that on suction side (upper surface) of wing. The higher pressure on lower surface meets the lower pressure on upper surface at the tip of wing, subsequently around the wingtip; a current of the air will appear from lower surface to the upper surface that is called tip vortex. This vortex takes energy from aircraft; therefore it defines as a drag. The aspect ratio of wing effects on tip vortex, for high aspect ratio wing the difference between pressure on upper and lower surfaces is lower at wingtip then the tip vortex is weaker and consequently induced drag is smaller. When the wing is near the ground the tip vortex is trapped by the ground and reduces the strength of vortices, it seems that the effective aspect ratio of the wing is greater than geometric aspect ratio [1].

The chord dominated ground effect mostly can increase lift force. When the wing approaches to the ground, a higher pressure (ram effect) is generated at lower surface of the wing that is called dynamic air cushion. For very low ground clearance (h/c) the air flow reaches to stagnate accordingly the highest pressure is appear at lower surface of the wing. At small ground clearance and very small or negative angle of attack, When the lower surface of wing is convex a suction effect is

created at bottom and pulled down the wing. This outcome can use for design of race car to control it at high speed. Normally, the wing of WIG crafts should have as flat as possible and positive of angle of attack [1].

Several initial experimental and computational techniques to calculate the lift by special shape of the body in ground proximity can be found in the references [2-4]. Yang *et al.* [5] worked on longitudinal stability of WIG craft respect to some design parameters such as wing section, wing plan form, stabilizer, and endplate. They showed that the s-shaped wing modifies longitudinal stability at certain angle of attack but lost a little lift compared to popular wing section like Clark-y. Also, they depicted a tail wing had more effect on center in pitch than center in height, because the tail position was out of ground effect. It was shown the aerodynamic centers of forward swept (FS) wing and reversed forward swept (RFS) wing is nearer to leading edge of wings contrast to rectangular wing one. The performance (L/D) of rectangular wing was lower RFS wing and greater than FS wing in extreme ground effect. The canard wing as a replacement for tail wing is an alternative design parameter for stability of WIG craft [6-7]. Li *et al.* [7] showed that the canard wing causes the aerodynamic centers shift to leading edge of main wing without changing the relationship between centers. This is an advantage for locating the center of gravity. The weak point of canard wing was reported on its height stability, although it has good behaviour on pitching stability. They established the drag force of the canard wing is lesser than tail wing that gives higher efficiency. Lee *et al.* [8] carried out the aerodynamic characteristics of rectangular wing with anhedral angle and endplates respect to different angles of attack and ground clearances. Three configurations were examined, clean wing, wing with endplate and wing with anhedral angle. The lift to drag ratio of the wing with anhedral angle was in the middle among them, additionally, its height static stability satisfied for all angle of attacks and ground clearances. They described that the variations of lift coefficient of wing with anhedral angle versus Reynolds numbers is the smallest, while for drag coefficient is the largest compared to other models. The planform of wing is a new challenge in design of WIG craft [9-10]. Yang and Yang [9] numerically analyzed two configurations of WIG craft, one with airplane concept and another with Lippisch concept. The main wing of airplane type was a rectangular wing, and a reverse forward swept wing was used for the Lippisch type. They found that the performance and stability of the Lippisch type WIG craft was better than of airplane type. The higher lift coefficient and lower drag coefficient were found for the Lippisch type at different ground clearance and angle of attack. The Lippisch type WIG craft can fly in and out of ground effect with acceptable height static stability.

This study tries to show the aerodynamic coefficients of a new compound wing configuration in ground effect. This compound wing is composed of three parts; a rectangular wing in the middle and two reverse taper wings with an anhedral angle at the sides. Lift and drag coefficients, lift to drag ratio, moment coefficient and center of pressure of the present compound wing were measured respect to ground clearances. The numerical simulation employed a three dimensional CFD using a finite volume scheme. A realizable $k-\epsilon$ turbulent model was used for the turbulent flow around the wing. For the validation, the aerodynamics forces were experimentally measured in the low speed wind tunnel at the Universiti Teknologi Malaysia (UTM-LST).

2.0 CFD NUMERICAL STUDY

Present numerical study was carried out by a model of a rectangular wing and a compound wing with NACA6409 airfoil section. The principal dimensions of wings (Figure 1) are shown in Table 1. These simulation were prepared with respect to different angle of attack and ground clearance (h/c), aspect ratio 1.25 and velocity of airflow 25.5 m/s. Ground level (h) is defined by the distance between trailing edge of wings center and ground surface. The numerical scheme considered a steady-state, incompressible by means of realizable $k-\epsilon$ turbulent model of the Navier-stokes equations for flow over wing surface. The CFD models applied fluent software and high speed computer. The transport equations for the turbulent kinetic energy (k) and turbulent dissipation energy (ϵ) are expressed as follows.

$$\frac{\partial}{\partial t}(\rho k) + \frac{\partial}{\partial x_j}(\rho k u_j) = \frac{\partial}{\partial x_j} \left[\left(\mu + \frac{\mu_t}{\sigma_k} \right) \frac{\partial k}{\partial x_j} \right] + G_k + G_b - \rho \epsilon - Y_M + S_k \tag{1}$$

and

$$\frac{\partial}{\partial t}(\rho \epsilon) + \frac{\partial}{\partial x_j}(\rho \epsilon u_j) = \frac{\partial}{\partial x_j} \left[\left(\mu + \frac{\mu_t}{\sigma_\epsilon} \right) \frac{\partial \epsilon}{\partial x_j} \right] + \rho C_1 S_\epsilon - \rho C_2 \frac{\epsilon^2}{k + \sqrt{\nu \epsilon}} + C_{1\epsilon} \frac{\epsilon}{k} C_{3\epsilon} G_b + S_\epsilon \tag{2}$$

$$C_1 = \max \left[0.43, \frac{\eta}{\eta + 5} \right], \eta = \frac{k}{\epsilon}, S = \sqrt{2 S_\theta S_y} \tag{3}$$

where S_k and S_ϵ are user-defined Source terms, $C_{1\epsilon}$, C_2 , $C_{3\epsilon}$, σ_k and σ_ϵ are the adaptable constants.

The aerodynamic coefficients and center of pressure in this numerical study were determined as follows:

$$C_L = \frac{L}{0.5 \rho U^2 A}, C_D = \frac{D}{0.5 \rho U^2 A}, C_M = \frac{M}{0.5 \rho U^2 A c}, \text{ and}$$

$$X_{cp} = 0.25 + \frac{C_M}{C_L \cos \alpha + C_D \sin \alpha}$$

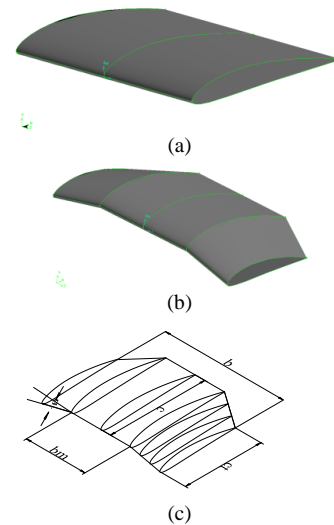


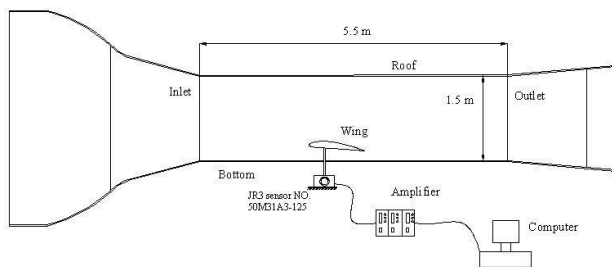
Figure 1 Types of wing configuration, (a) Rectangular wing, (b) Compound wing, (c) Geometry of the compound wing

Table 1 Principal dimension of rectangular wing and compound wings with different middle wing span

Dimension	Rectangular wing	Compound wing
Total wing span (b)	250 mm	250 mm
Root chord length (c)	200 mm	200 mm
Middle wing span (b_m)	-	125
Taper ratio (c/c)	-	1.25
Anhedral angle (α)	-	13°

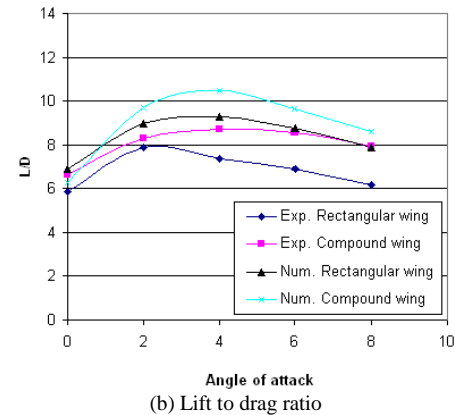
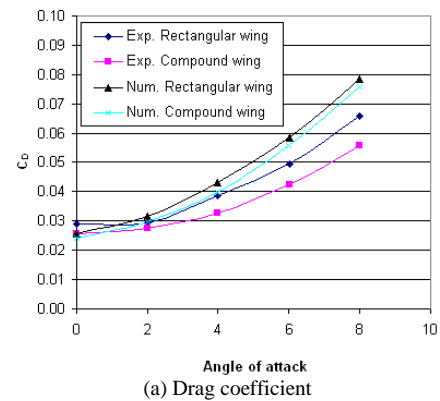
3.0 EXPERIMENTAL PROCEDURES AND SET-UP

In the wind tunnel, aerodynamic force measurements were carried out respect to ground clearances (h/c) and angles of attacks (α). Ground clearance (h/c) was defined as the distance ratio between the wing trailing edge center and ground surface (h) to root chord length (c) of the wing. Figure 2 shows the experimental setup of current experiment in the low speed wind tunnel at the Universiti Teknologi Malaysia (UTM-LST).

**Figure 2** Experimental setup in the low speed wind tunnel at the Universiti Teknologi Malaysia

4.0 TENDENCY OF NUMERICAL AND EXPERIMENTAL SIMULATIONS

In this project, according to numerical and experimental simulations it can be seen that the results of both simulations have similar trend. Figure 3a-b shows the aerodynamic coefficients of the rectangular and the compound wings at ground clearance of 0.15. The numerical results had some deviations from experiments but both simulations show the compound wings have some improvements in aerodynamic performance compared to the rectangular wing at small ground clearance. Also, both simulations confirmed that drag coefficient of compound wing was smaller that of the rectangular wing at small ground clearance and angle of attack greater than 2°, and lift to drag ratio of the compound wing was greater as well. It is important that the experiments validated the performance of the compound wing where there are some improvements at low ground clearances. In validation purpose, the experimental results confirmed the compound wing is suitable configuration to employ in WIG crafts for flying near the ground.

**Figure 3** Comparison of experimental and numerical simulation results at ground clearance of 0.15, (a) Drag coefficient, (b) Lift to drag ratio

5.0 RESULTS AND DISCUSSIONS

5.1 Pressure and Velocity Contours

Figures 4-9 show the pressure and velocity distribution of compound wing (Table 1) at ground clearances of 0.1 and 0.4 with angle of attack of 4°. Figure 4 demonstrates the suction effect on the upper surface of compound wing at ground clearance of 0.1 is slightly stronger. There is a higher pressure near leading edge of upper surface at ground clearance of 0.4 that means the stagnation point is nearer to leading edge at this height (Figure 4b). The higher pressure distribution on lower surface of the compound wing shows the pressure increased in lower side of the compound wing at ground clearance of 0.1 (Figure 4a). At lower ground clearance, there is higher pressure in flow passage between lower side of compound wing and ground at middle span as shown in Figures 5-6, also the stagnation point moves to lower side of compound wing as wing approaches to ground. Figures 7-8 depict higher velocity in flow passage under compound wing at ground clearance of 0.4. The pressure distribution near wingtip of the compound wing at ground clearance of 0.1 (Figures 9a) indicates that its tip vortices are gradual weaker compared to higher ground clearance (Figure 9b), therefore, the induced drag of the compound wing dropped when ground clearance was decreased.

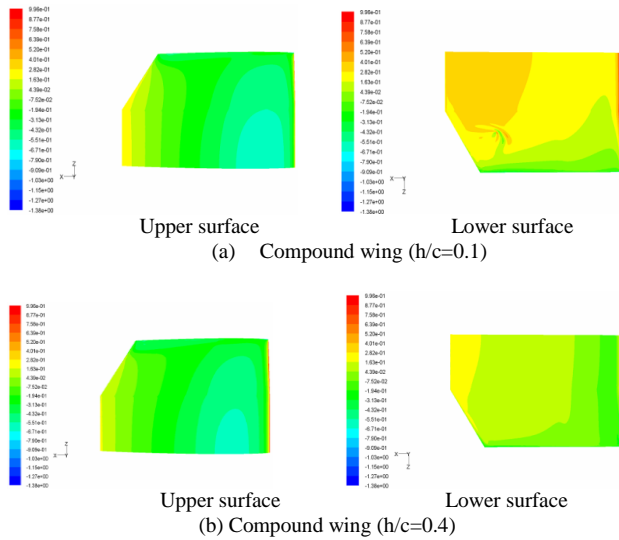


Figure 4 Pressure coefficient contour on upper and lower surface of compound wing at ground clearances of 0.1 and 0.4 with angle of attack of 4°

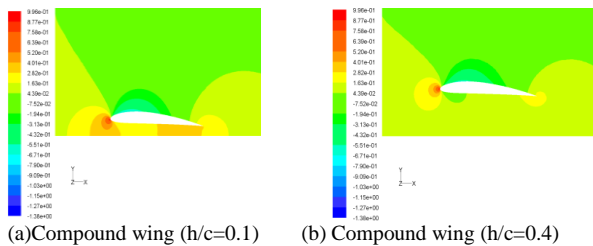


Figure 5 Pressure coefficient contour on the middle span of compound wing at ground clearances of 0.1 and 0.4 with angle of attack of 4°

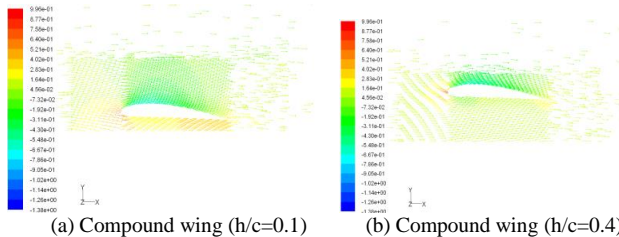


Figure 6 Velocity vector colored by pressure coefficient on the middle span of compound wing at ground clearances of 0.1 and 0.4 with angle of attack of 4°

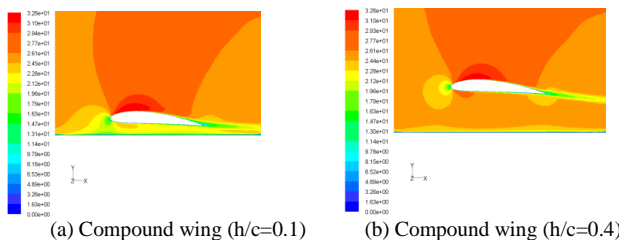


Figure 7 Velocity contour (m/s) on the middle span of compound wing at ground clearances of 0.1 and 0.4 with angle of attack of 4°

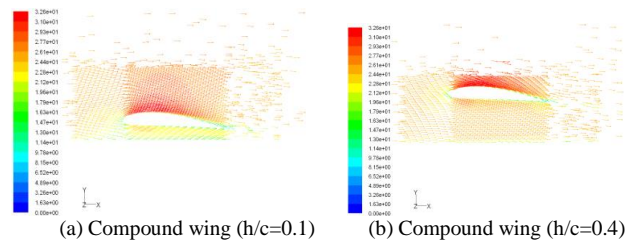


Figure 8 Velocity vector colored by velocity magnitude (m/s) on the middle span of compound wing at ground clearances of 0.1 and 0.4 with angle of attack of 4°

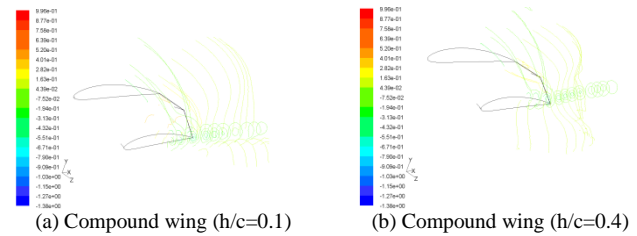


Figure 9 Pressure coefficient distribution near wingtip of compound wing at ground clearances of 0.1 and 0.4 with angle of attack of 4°

5.2 Lift Coefficient

The effect of different ground clearance on aerodynamic coefficients of the rectangular wing and the compound wing (Table 1) at angle of attack of 4° is shown in Tables 2-6 and Figures 10-14. Figure 10 illustrates quick increase in the lift coefficients of both wings as ground clearance was decreased specially at ground clearance lower than of 0.2. The compound wing has a favorable enhancement where the plot of lift coefficient of the compound wing is upper than that of the rectangular wing. According to the present results the decreasing of ground clearance could improve considerably the ram pressure on lower surface of the compound wing. The increment of lift coefficient of the compound wing compared with rectangular wing was calculated by Equation 4 and summarized in Table 2. The increments have substantial value at small ground clearance where at ground clearance of 0.1 is 17.3%.

$$Increment(\%) = \frac{C_{L(Compound)}}{C_{L(Rectangular)}} - 1 \tag{4}$$

Table 2 Lift coefficient and its increment versus ground clearance at angle of attack of 4° for rectangular wing and compound wing

Ground clearance	Lift coefficient		Increment of CL (%)
	Rectangular wing	Compound wing	
0.1	0.428	0.502	17.3
0.15	0.400	0.416	4.0
0.2	0.384	0.385	0.4
0.3	0.364	0.353	-3.0
0.4	0.352	0.337	-4.2

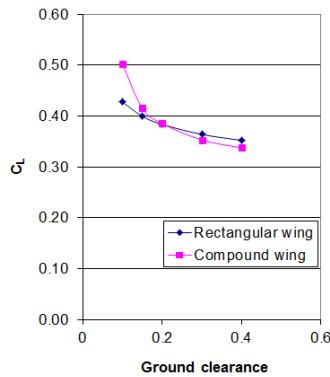


Figure 10 Lift coefficient (C_L) versus ground clearance at angle of attack of 4°

5.3 Drag Coefficient

The drag coefficients of the rectangular wing and the compound wing (Table 1) versus ground clearance are depicted in Figure 11; in addition the reduction of drag coefficient of the compound wing was calculated by Equation 5 in Table 3. Figure 11 reveals a small variation in the drag coefficient of both wings with increase ground clearance; however, the drag coefficient of the compound wing had some fluctuation. The plot of the compound wing is considerable lower that of the rectangular wing. The weaker tip vortex of the compound wing is main reason of the reduction in its drag coefficient compared to the rectangular wing. As mentioned before, smaller ground level and area of the tip of the compound wing causes weaker tip vortex. The reduction of drag coefficient is between 5.9-8.6% as shown in Table 3.

$$Reduction(\%) = 1 - \frac{C_{D(Compound)}}{C_{D(Rectangular)}} \quad (5)$$

Table 3 Drag coefficient and its reduction versus ground clearance at angle of attack of 4° for rectangular wing and compound wing

Ground clearance	Drag coefficient		Reduction of CD (%)
	Rectangular wing	Compound wing	
0.1	0.0430	0.0405	5.9
0.15	0.0430	0.0397	7.8
0.2	0.0430	0.0400	6.8
0.3	0.0432	0.0395	8.6
0.4	0.0433	0.0407	6.0

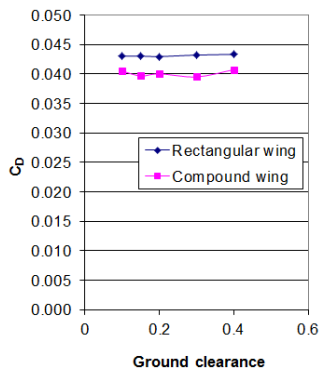


Figure 11 Drag coefficient (C_D) versus ground clearance at angle of attack of 4°

5.4 Lift to Drag Ratio

The lift to drag ratio of the rectangular wing and the compound wing (Table 1) versus ground clearance was summarized in Table 4, in addition, the increment of lift to drag ratio of the compound wing was determined by Equation 6. The increment of lift to drag ratio of the compound wing is noticeable at all ground clearance as compared with the rectangular wing, for example, at ground clearance of 0.1, this increment is 24.7%. The trend of lift to drag ratio of the compound wing and the rectangular wing versus ground clearance is shown in Figure 12. The plot of the compound wing is upper especially at low ground clearance, that means the efficiency of the compound wing significantly is higher that of the rectangular wing.

$$Increment(\%) = \frac{L/D_{(Compound)}}{L/D_{(Rectangular)}} - 1 \quad (6)$$

Table 4 Lift to drag ratio and its increment versus ground clearance at angle of attack of 4° for rectangular wing and compound wing

Ground clearance	Lift to drag ratio		Increment of L/D (%)
	Rectangular wing	Compound wing	
0.1	9.93	12.39	24.7
0.15	9.29	10.48	12.8
0.2	8.93	9.63	7.8
0.3	8.42	8.94	6.2
0.4	8.13	8.29	1.9

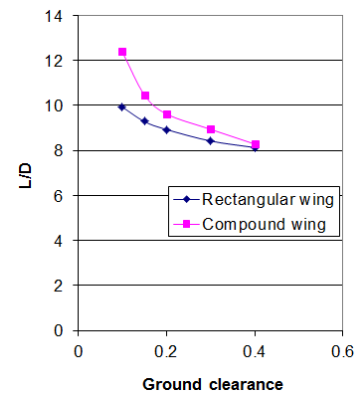


Figure 12 Lift to drag ratio (L/D) versus ground clearance at angle of attack of 4°

5.4 Moment Coefficient and Center of Pressure

The variation of moment coefficients of the rectangular wing and the compound wing (Table 1) versus ground clearance is shown in Table 5 and Figure 13. A moment coefficient that causes a decreasing on angle of attack was defined as a positive moment. The trend of moment coefficients in Figure 13 indicates the increasing of ground clearance causes a drop in moment coefficient and stability of the compound wing and the rectangular wing, although the rate of this decline is higher for the compound wing at low ground clearance. These differences mostly could be related to pressure distribution of wing surface and subsequently center of pressure. The reduction of moment coefficient of the compound wing was calculated by Equation 7 in Table 5. This reduction is small at low ground clearance

where it is 3.2% at ground clearance of 0.1, however, it increases rapidly by raising the ground clearance. In Table 6, the reduction of distance of center of pressure from leading edge of the compound wing was calculated by Equation 8, this reduction is between 7-8%. Based on present results the moving of the center of pressure of the compound wing and the rectangular wing is small with respect to variation of ground clearance as shown in Figure 14.

$$\text{Increment}(\%) = 1 - \frac{C_{M(\text{Compound})}}{C_{M(\text{Rectangular})}} \quad (7)$$

$$\text{Reduction}(\%) = 1 - \frac{X_{CP}/c_{(\text{Compound})}}{X_{CP}/c_{(\text{Rectangular})}} \quad (8)$$

Table 5 Moment coefficient and its reduction versus ground clearance at angle of attack of 4° for rectangular wing and compound wing

Ground clearance	Moment coefficient		Reduction of C_M (%)
	Rectangular wing	Compound wing	
0.1	0.075	0.073	3.2
0.15	0.072	0.061	15.9
0.2	0.069	0.057	18.2
0.3	0.065	0.052	20.6
0.4	0.060	0.047	21.0

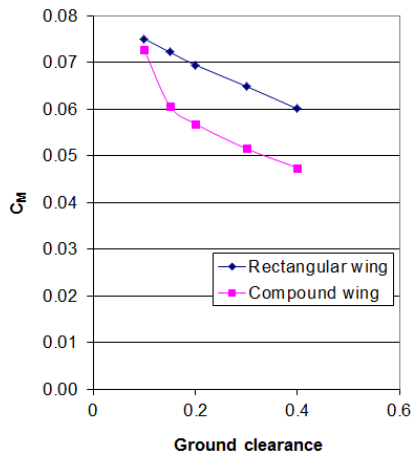


Figure 13 Moment coefficient (CM) versus ground clearance at angle of attack of 4°

Table 6 Center of pressure and its reduction versus ground clearance at angle of attack of 4° for rectangular wing and compound wing

Ground clearance	Center of pressure		Reduction of X_{CP}/c (%)
	Rectangular wing	Compound wing	
0.1	0.425	0.394	7.2
0.15	0.430	0.395	8.0
0.2	0.430	0.397	7.7
0.3	0.427	0.395	7.5
0.4	0.419	0.390	7.1

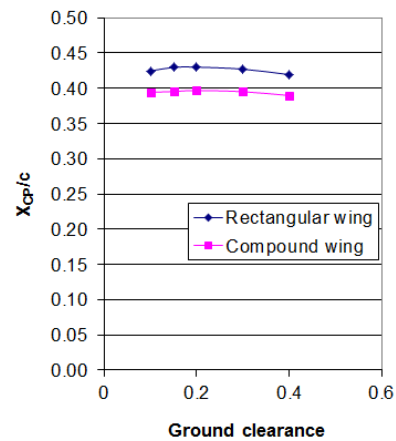


Figure 14 Center of pressure (X_{CP}/c) versus ground clearance at angle of attack of 4°

6.0 CONCLUSION

The aerodynamic characteristics of a compound wing were numerically investigated. The compound wing is divided into three parts; the middle part as the rectangular wing and two side parts that are reverse taper wing with an anhedral angle. The excellent performance of compound wing was in small ground clearance ($h/c < 0.2$). There was favorable increment of the lift coefficient in small ground clearance, although, drag coefficient had no more variation with ground clearance but lift to drag ratio of compound wing had substantial improvement. At small ground clearance, there was high ram effect and low tip vortex for the compound wing compared to the rectangular wing. The reduction of moment coefficient of compound wing was faster than that of the rectangular wing as ground clearance of wings was decreased. Also, the percentage of this reduction was higher for the compound wing. Meanwhile, the position of center of pressure of both compound and rectangular wings had small fluctuation respect to ground clearance. The center of pressure of the compound wing was nearer to leading edge compared to the rectangular wing

Acknowledgement

The authors would like to thank the Ministry of Science, Technology, and Innovation (MOSTI) Malaysia for funding this research.

References

- [1] Abramowski, T. 2007. Numerical Investigation of Airfoil in Ground Proximity. *Journal of Theoretical and Applied Mechanics*. 45(2): 425–436.
- [2] Davis, J. E., and G. L. Harris. 1973. Nonplanar Wings in Nonplanar Ground Effect. *Journal of Aircraft*. 10(5): 308–312.
- [3] Barrows, T. M. 1973. The Ram Air Cushion-advanced Fluid Suspension for Tracked Levitated Vehicles. ASME 73-ICT-14.
- [4] Widnall, S. E., and T. M. Barrows. 1970. An Analytic Solution for Two and Three-Dimensional Wings in Ground Effect. *Journal of Fluid Mechanics*. 41(4): 769–792.
- [5] Yang, W., Z. Yang, and C. Ying. 2010. Effects of Design Parameters on Longitudinal Static Stability for WIG craft. *International Journal of Aerodynamics*. 1(1): 97–113.
- [6] Li, Y., W. Yang, and Z. Yang. 2010. Numerical Study on wing in Ground Effect of Canard Configuration. *Aeronautical Computing Technique*. 40(4): 27–30.

- [7] Li, Y., W. Yang, and Z. Yang. 2010. Numerical study on static Longitudinal Stability of Canard WIG Craft. *Flight Dynamics*. 28(1): 9–12.
- [8] Lee, J., C. S. Han, and C. H. Bae. 2010. Influence of Wing Configurations on Aerodynamic Characteristics of Wings in Ground Effect. *Journal of Aircraft*. 47(3): 1030–1040.
- [9] Yang, W., and Z. Yang 2009. Aerodynamic Investigation of a 2D Wing and Flows in Ground Effect. *Chinese Journal of Computational Physics*. 26(2): 1–240.
- [10] Ying, C., W. Yang, and Z. Yang. 2010. Numerical Simulation on Reverse Forward Swept Wing in Ground Effect. *Computer Aided Engineering*. 19(3): 35–39.